

Kinetic Studies on the Photochemically Activated Solvation of $[(\eta^6\text{-arene}_1)\text{Ru}(\eta^6\text{-arene}_2)]^{2+}$ Sandwich Compounds

Thomas Karlen, Andreas Hauser, and Andreas Ludi*

Institut für Anorganische Chemie, Universität Bern, CH 3000 Bern 9, Switzerland

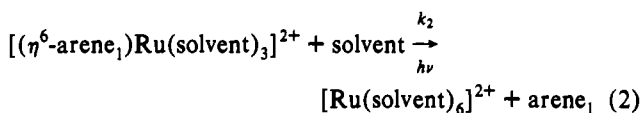
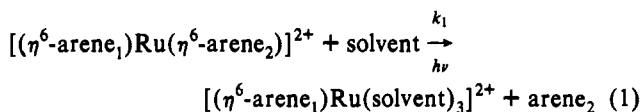
Received November 4, 1993*

Irradiation of the inert complexes $[(\eta^6\text{-arene}_1)\text{Ru}(\eta^6\text{-arene}_2)]^{2+}$ (arene = benzene, toluene, mesitylene, hexamethylbenzene, anisole, biphenyl, naphthalene, chrysene) in various solvents ($\text{H}_2\text{O}/\text{H}^+$, $\text{H}_2\text{O}/\text{H}^+/\text{EtOH}$, acetonitrile, DMSO) leads to the fully solvated complexes $[\text{Ru}(\text{solvent})_6]^{2+}$. The reaction occurs in two consecutive steps. The first step is the formation of the intermediate $[(\eta^6\text{-arene})\text{Ru}(\text{solvent})_3]^{2+}$ with either arene₁ or arene₂ being replaced by solvent. The linear dependence of the observed rate constant for the first step on concentration of solvent as well as reactant is consistent with a second-order reaction. The formation of the half-sandwich intermediates depends on substituents on the arene, irradiation wavelength, temperature, and solvent. The magnitude of the quantum yields Φ_p is rationalized in terms of steric and electronic effects. The sequence for the release of arenes in the nonsymmetrically substituted complexes as monitored by $^1\text{H-NMR}$ is shown to be consistent with a simple MO view, based on overlap strength in the electronic ground state of the starting compound. Luminescence properties of $[(\text{C}_6\text{Me}_6)_2\text{Ru}](\text{tos})_2$ (tos = *p*-toluenesulfonate) are used for deriving information about the excited state.

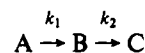
Introduction

Fully or partially solvated complexes of Ru(II) formed in situ from inert ruthenium arene compounds are of potential use in small-scale preparative organometallic chemistry for the generation of labile, well-defined starting materials or as precursors in catalytic processes. With this route, the sometimes complicated synthesis and delicate handling of species such as $[\text{Ru}(\text{H}_2\text{O})_6]^{2+}$ and $[\text{Ru}(\text{DMF})_6]^{2+}$ (DMF = *N,N*-dimethylformamide) can be avoided.

The study of thermal and photochemical reactions of sandwich compounds has attracted considerable interest in the course of the last 10 years. Solvation can be induced by irradiation with light. $[\text{CpRu}(\eta^6\text{-arene})]^+$ (Cp = C_5H_5^-) and $[(\eta^6\text{-arene})\text{Ru}(\text{solvent})_3]^{2+}$ produce photochemically stable $[\text{CpRu}(\text{solvent})_3]^+$ or $[\text{Ru}(\text{solvent})_6]^{2+}$, respectively.^{1,2} A thermal pathway was observed for bis(arene) complexes with one condensed aromatic ligand, e.g. $[(\eta^6\text{-C}_6\text{Me}_6)\text{Ru}(\eta^6\text{-arene})]^{2+}$ and $[(\eta^6\text{-C}_6\text{H}_3\text{Me}_3)\text{Ru}(\eta^6\text{-arene})]^{2+}$ or $[\text{CpRu}(\eta^6\text{-arene})]^+$. Arene represents naphthalene, anthracene, pyrene, chrysene, or azulene.^{3–5} We investigated the quantitative aspects of the photochemistry of a series of symmetrically and unsymmetrically substituted Ru(II) sandwich compounds. In particular, we are interested in the first of the two consecutive steps in the solvation process



or schematically



To our knowledge, the literature contains no quantitative information concerning reaction 1. For this reason, our study is a complementary extension of work published by Weber and Ford.²

Experimental section

Materials and Preparation. All of the compounds $[(\eta^6\text{-arene}_1)\text{Ru}(\eta^6\text{-arene}_2)](\text{BF}_4)_2$ and $[(\eta^6\text{-arene}_1)\text{Ru}(\eta^6\text{-arene}_2)](\text{tos})_2$ (tos = *p*-toluenesulfonate) were obtained by the method of Bennett and Matheson⁴ or by refluxing $[(\eta^6\text{-C}_6\text{H}_6)\text{Ru}(\text{H}_2\text{O})_3](\text{tos})_2$ in CF_3COOH with excess of arene₂.⁶ Throughout, reagent grade chemicals were used. All products are inert toward oxidation both as solids and in solutions used for measurements. No thermal decomposition of the dissolved compounds could be observed under the conditions of our experiments. Solutions were prepared under air in red light and stored in the dark to prevent induction of the reaction by daylight. $[(\text{C}_6\text{D}_6)_2\text{Ru}](\text{BF}_4)_2$ was obtained by a variation of a procedure described by Fischer⁷ for the synthesis of $[(\text{C}_6\text{H}_6)_2\text{Ru}](\text{PF}_6)_2$ using $\text{Na}(\text{BF}_4)$ as source of the counterion. All products were characterized by elemental analysis and NMR or UV spectroscopy. The complexes referred to as I–X are listed in Table 1.

Photochemical Procedures. A 1-cm quartz cuvette containing a solution of the bis(arene) complex (2.0 mL, 1.0×10^{-3} M or less) in the appropriate solvent was saturated with argon to prevent oxidation of photolysis products. This magnetically stirred solution was irradiated using an argon laser (Spectra-Physics 2045) with irradiation wavelength $\lambda_{\text{irr}} = 458, 364,$ or 351 nm. The optical density of the solutions at the irradiation wavelengths was chosen as 0.3 or less. Thus the amount of excited state is proportional to the concentration of the absorber. The reaction mixture was thermostated to 25 ± 0.1 °C if not stated otherwise. The light intensity was held constant by running the laser in the power lock mode. Incident irradiation intensity was measured with an electronic power meter. The reaction was followed by monitoring either the decrease of extinction for the lowest energy absorption band of A (IX, X) or the intensity change around 400 nm caused by intermediate B (I–VIII) as a function of irradiation time. Electronic spectra were recorded on a diode array spectrophotometer (HP 8451A).

In the course of the reaction, aqueous solutions became turbid, owing to the insolubility of free arenes (mesitylene, naphthalene, etc.). In order to prevent formation of heterogeneous systems, most experiments were carried out in H_2O (0.05 M H_2SO_4)/EtOH (3/2), allowing thus

* Abstract published in *Advance ACS Abstracts*, April 1, 1994.
 (1) Schrenk, J. L.; McNair, A. M.; McCormick, F. B.; Mann, K. R. *Inorg. Chem.* **1986**, *25*, 3501.
 (2) Weber, W.; Ford, P. C. *Inorg. Chem.* **1986**, *25*, 1088.
 (3) Freedman, D. A.; Mann, K. R. *Inorg. Chem.* **1989**, *28*, 3920.
 (4) Bennett, M. A.; Matheson, T. W. *J. Organomet. Chem.* **1979**, *175*, 87.
 (5) McNair, A.; Mann, K. R. *Inorg. Chem.* **1986**, *25*, 2519.

(6) Stebler-Röthlisberger, M.; Hummel, W.; Pittet, P.-A.; Bürgi, H.-B.; Ludi, A.; Merbach, A. E. *Inorg. Chem.* **1988**, *27*, 1358.
 (7) Fischer, E. O.; Elschenbroich, Ch. *Chem. Ber.* **1970**, *103*, 162.

comparable measurements over the whole series of I–X. The acid prevented hydrolysis of $[\text{Ru}(\text{H}_2\text{O})_6]^{2+}$ and served to approximately define the ionic strength of the medium.

The leaving arene group in reaction 1 was identified by $^1\text{H-NMR}$ spectroscopy. Argon-saturated concentrated solutions of I–X in the appropriate solvents were irradiated in the NMR tubes at 364 nm. DMSO- d_6 or acetone- d_6 was added to increase the solubility of A. Spectra were recorded with a Bruker AC 300 at variable intervals and compared to reference spectra of the pure compounds.

Luminescence measurements were performed either on powder samples or on foils of poly(methyl methacrylate) PMMA (about 1% in weight of bis(arene) complex). For low-temperature measurements (5–125 K) a flow tube technique was used. An argon laser (Spectra-Physics 2045) was used for excitation at 364 nm (5–10 mW). The emission was dispersed by a double monochromator (Spex 1402) and measured by a photon-counting system (Stanford Research SR400). For lifetime measurements a pulsed Nd-YAG laser (Spectra Physics DCR-3; 351 nm, 100 $\mu\text{J}/\text{pulse}$) was used.

Extended Hückel calculations were done on a VAX computer with an update version of the program ICON. Parameters for Ru(II) in metal-organic compounds were taken from the literature.⁸ There exist only crystal structures for I⁹ and VI.¹⁰ As the average distance Ru–C_{arene} increases by only 0.04 Å upon permethylation, Ru–C_{arene} = 2.221 Å was taken as in I for all calculations. Eclipsed conformation was assumed for all sandwich complexes. Bond distances in the ligands were taken from crystal structures of the free arenes.¹¹ Calculations on VIII and X were omitted. These ligands show too many degrees of freedom.

Results and Discussion

Rate Law. The appearance and disappearance of an intense absorption band around 400 nm during the photolysis of A indicate the formation of half-sandwich species B as intermediates. In order to describe the kinetics of reaction 1, the partial orders α and β with respect to reactant A and solvent have to be obtained. The reaction rate of (1) is expressed by

$$V = d[\text{B}]/dt = k[\text{A}]^\alpha[\text{solvent}]^\beta \quad (3)$$

α may be derived by utilizing a large excess of solvent. This is always the case in our experiments, and therefore (3) simplifies to

$$V = k'[\text{A}]^\alpha \quad (k' = k[\text{solvent}]^\beta = \text{const}) \quad (4)$$

If $\alpha = 1$ and measurements are performed at low conversion and constant irradiation power, the observed rate constant k_{obs} must be proportional to $[\text{A}]_0$. In the photolysis of I (0.05 M $\text{H}_2\text{SO}_4/0.1$ M NaBF_4 , $\lambda_{\text{irr}} = 364$ nm, 44 mW) the increase of k_{obs} with $[\text{A}]_0$ ranging from 3.04×10^{-4} to 6.3×10^{-3} M is linear with a correlation coefficient of $R^2 = 0.995$. No salt effect is observed upon change of medium to 0.05 M H_2SO_4 . A slight increase of k_{obs} in a water/ethanol mixture may be attributed to enhanced solubility of reaction products. Inspection of (4) shows, that k_{obs} is proportional to solvent concentration if $\beta = 1$. The test for the influence of the solvent concentration was carried out with I in DMSO because of the very good solubility of the sandwich compound in this medium. "Diluting" with toluene without precipitation of reactant was possible down to $[\text{DMSO}] = 3.52$ M. A linear dependence of k_{obs} on $[\text{DMSO}]$ ($R^2 = 0.994$, $\lambda_{\text{irr}} = 364$ nm, 100 mW) was obtained with a nonvanishing intercept at $[\text{DMSO}] = 0$ probably due to weak nucleophilic character of the diluant. From the slope a second-order rate constant of $1.2 \times 10^{-4} \text{ M}^{-1} \text{ s}^{-1}$ was derived. As k_{obs} is proportional to the concentration of reactant and solvent, (1) is shown to be of pseudo first order (solvent in large excess).

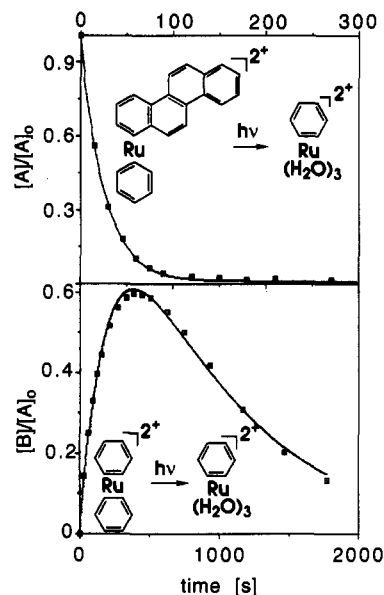


Figure 1. Examples for time-dependent concentrations of A and B in photolysis experiments: (top) decrease of X and fit of data points using formula 5; (bottom) formation and disappearance of the intermediate half-sandwich $[(\text{C}_6\text{H}_6)\text{Ru}(\text{H}_2\text{O})_3]^{2+}$ in the photolysis of VII and fit to formula 6.

Solving the differential equations for a two-step reaction with each step being of pseudo first order leads to the following analytical expressions for the time-dependent concentrations of A and B, which are exact for low optical density and negligible product absorption:

$$[\text{A}] = [\text{A}]_0 \exp(-k_1 t) \quad (5)$$

$$[\text{B}] = [\text{A}]_0 k_1 / (k_2 - k_1) [\exp(-k_1 t) - \exp(-k_2 t)] \quad (6)$$

In principal, rate constants can be obtained by nonlinear fits using expression 5 in the photolysis of IX and X or expression 6 for I–VIII (see Figure 1). But in order to exclude internal filter effects resulting from the absorbance of product at the irradiation wavelength, values for k_1 were determined at low conversion (see Table 1). Of course, the apparent rate constant k_1 is proportional to the intensity of irradiation ($R^2 = 0.993$ for I_0 ranging from 50 mW to 250 mW).

A marked sensitivity of the reaction to the nucleophilicity of solvent molecules was observed. The second-order rate constant for the photolysis of I in acetonitrile or in DMSO is about 10 times larger than the one for photolysis in water. This is consistent with nucleophilic attack at the metal center of the excited bis(arene) complex as the rate-determining step. Complete photolysis in acetonitrile yields $[\text{Ru}(\text{AN})_6]^{2+}$ as characterized by its UV/vis spectrum.

No isosbestic points as indicators for a well-defined reaction were observed during the laser photolysis of I–III and VII because of the similar magnitudes of k_1 and k_2 . However, it was possible to obtain isosbestic points for the photolysis of VIII–X at $\lambda_{\text{irr}} = 458$ nm due to the low quantum yield of reaction 2 at higher wavelength² (see Figure 2). Likewise, isosbestic points appeared in the photolysis of IV–VI at all excitation wavelengths. With these reactants, a very slow replacement of the second arene takes place.

Calculation of Φ_p . Quantum yields Φ_p for the first reaction step (1) were calculated from the rate constants k_1 . With a three-level scheme, including ground state, excited state, and thermally equilibrated excited state, the following set of differential equations can be derived:

(8) Amouyal, E.; Mouallem-Bahout, M.; Calzaferri, G. *J. Phys. Chem.* **1991**, *95*, 7641.

(9) Beck, U.; Hummel, W.; Bürgi, H. B.; Ludi, A. *Organometallics* **1987**, *6*, 20.

(10) Ward, M. D.; Johnson, D. C. *Inorg. Chem.* **1987**, *26*, 4213.

(11) Wyckoff, R. W. G. *Crystal Structures*, 2nd ed.; Interscience Publishers: New York, 1971; Vol. 6.

Table 1. Quantum Yields Φ_p at Different Wavelengths for Arene Labilization in $[(\text{arene})_1\text{Ru}(\text{arene})_2]^{2+}$

no.	compd	$10^3 k_1, \text{s}^{-1} \text{ }^a$	$10^2 \Phi_p^{b,c}$			$\lambda_{\text{obs}}, \text{nm}$
			351 nm	364 nm	458 nm	
I	$[(\text{C}_6\text{H}_6)_2\text{Ru}](\text{BF}_4)_2$	3.2 (2)	5.4(5)	10(1)	<i>d</i>	400
II	$[(\text{C}_6\text{H}_6)\text{Ru}(\text{C}_6\text{H}_5\text{Me})](\text{BF}_4)_2$	3.1(3)	<i>e</i>	8.7(5)	<i>d</i>	400
III	$[(\text{C}_6\text{H}_6)\text{Ru}(1,3,5\text{-C}_6\text{H}_3\text{Me}_3)](\text{BF}_4)_2$	3.0(1)	<i>e</i>	7.8(2)	<i>d</i>	400
IV	$[(\text{C}_6\text{H}_6)\text{Ru}(\text{C}_6\text{Me}_6)](\text{BF}_4)_2$	2.8(2)	<i>e</i>	6.6(4)	<i>d</i>	400
V	$[(1,3,5\text{-C}_6\text{H}_3\text{Me}_3)\text{Ru}(\text{C}_6\text{Me}_6)](\text{BF}_4)_2$	0.08	<i>e</i>	0.17	<i>d</i>	400
VI	$[(\text{C}_6\text{Me}_6)_2\text{Ru}](\text{BF}_4)_2$	0.1	<i>e</i>	0.21	<i>d</i>	400
VII	$[(\text{C}_6\text{H}_6)\text{Ru}(\text{C}_6\text{H}_5\text{OMe})](\text{BF}_4)_2$	1.1(3)	5.3(4)	1.5(5)	<i>d</i>	400
VIII	$[(\text{C}_6\text{H}_6)\text{Ru}(\text{biphenyl})](\text{BF}_4)_2$	6.7(4)	1.6(3)	2.0(3)	7.8(5)	420
IX	$[(\text{C}_6\text{H}_6)\text{Ru}(\text{naphthalene})](\text{BF}_4)_2$	24(3)	4.0(3)	4.6(6)	2.0(2)	450
X	$[(\text{C}_6\text{H}_6)\text{Ru}(\text{chrysene})](\text{BF}_4)_2$	152(12)	7.4(4)	2.4(4)	22(10)	450

^a Pseudo-first-order rate constant k_1 for reaction 1 determined at low conversion ($\lambda_{\text{irr}} = 364 \text{ nm}$, 200 mW). ^b Solvent H_2O (0.05 M H_2SO_4)/EtOH (3/2). All solutions $1.0 \times 10^{-3} \text{ M}$ except [VIII]–[X] $< 1.0 \times 10^{-4} \text{ M}$. ^c Determination of errors by at least three independent measurements except for V and VI because of very slow reaction. ^d Very small. ^e Not measured.

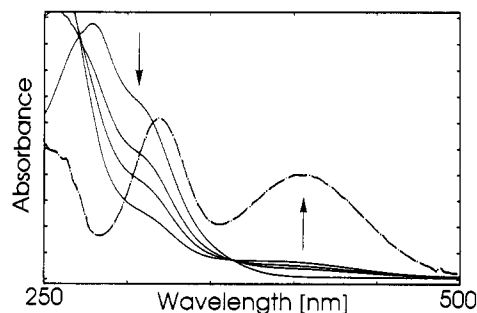


Figure 2. Photolysis of IX ($\lambda_{\text{irr}} = 458 \text{ nm}$) in H_2O (0.05 M H_2SO_4)/EtOH (3/2). Dotted line: Absorption spectrum of $[(\text{C}_6\text{H}_6)\text{Ru}(\text{H}_2\text{O})_3]^{2+}$ (tos)₂ (enlarged).

$$d[\text{A}]/dt = -k_{\text{ex}}[\text{A}] + k_{\text{nr}}[\text{A}^*] = -k_1[\text{A}]$$

$$d[\text{A}^*]/dt = k_{\text{ex}}[\text{A}] - (k_{\text{nr}} + k_p)[\text{A}^*]$$

$$d[\text{B}]/dt = k_p[\text{A}^*] - k_2[\text{B}]$$

A and A* are reactant ground state and excited state, respectively, k_{nr} is the rate constant for nonradiative relaxation back to A, and k_p is the rate constant for product formation. For low laser power $[\text{A}^*] \ll [\text{A}]$ and therefore $d[\text{A}^*]/dt \approx 0$.

$$[\text{A}^*] = [\text{A}]k_{\text{ex}}/(k_{\text{nr}} + k_p)$$

$$d[\text{A}]/dt = -k_{\text{ex}}[\text{A}]k_p/(k_{\text{nr}} + k_p) = -k_{\text{ex}}\Phi_p[\text{A}]$$

$$\Phi_p = k_p/(k_{\text{nr}} + k_p) = k_1/k_{\text{ex}} \quad (7)$$

$k_{\text{ex}} = \sigma_\lambda F$ is the excitation rate constant with $F = I/h\nu$ being the photon flux and $\sigma_\lambda = (3.8236 \times 10^{-21})\epsilon_\lambda$ (σ_λ is the absorption cross section at the excitation wavelength).¹² With low optical density, $I \approx I_0$ across the cell and k_{ex} is approximately constant. Quantum yields for the photolysis of I–X are summarized in Table 1.

The setup and the calculations for Φ_p were tested on the reaction $[\text{Ru}(\text{C}_6\text{H}_6)(\text{H}_2\text{O})_3]^{2+} + 3\text{H}_2\text{O} + h\nu \rightarrow [\text{Ru}(\text{H}_2\text{O})_6]^{2+}$ already studied.² The reported value, $\Phi_p = 1.4(1) \times 10^{-2}$ ($\lambda_{\text{irr}} = 366 \text{ nm}$), agrees with our determination $\Phi_p = 1.2(2) \times 10^{-2}$ ($\lambda_{\text{irr}} = 364 \text{ nm}$).

Dissociation Sequence of Ligands. ¹H-NMR spectroscopy can be used to discriminate between bound and free arene in the course of reactions 1 and 2. Identification is straightforward for highly symmetrical molecules like I and III–VI, and supported by reference spectra for the other systems. With increasing irradiation time, resonances for arenes in half-sandwiches with their typical shift to higher field show up. After exhaustive photolysis, only signals for free arenes remain. Reaction 1 as

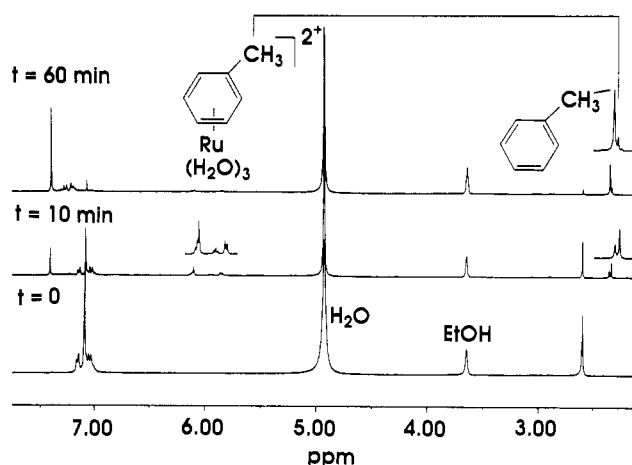
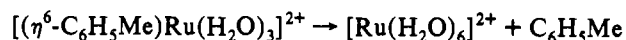
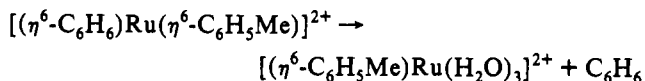


Figure 3. Photolysis of II in D_2O /ethanol- d_6 in an NMR tube. Spectra: (bottom) before irradiation; (middle) after 10 min and (top) after 60 min of irradiation at 364 nm (100 mW). A signal for free benzene is growing at 7.4 ppm simultaneously with a multiplet around 6 ppm, indicating intermediate formation of $[(\text{C}_6\text{H}_5\text{Me})\text{Ru}(\text{H}_2\text{O})_3]^{2+}$. The methyl region shows the toluene in the half-sandwich at 2.328 ppm and free toluene at 2.345 ppm.

well as reaction 2 is irreversible; the spectra of partially photolyzed samples containing A, B, and free arene do not change if the samples are stored for 2 d in the dark under an argon atmosphere.

With the unsymmetrically substituted sandwich compounds, two products B can be formed, depending on which of the two nonidentical arenes is replaced by solvent first. Figure 3 shows the photolysis of II. Parallel to the decrease of the signals belonging to $[(\eta^6\text{-C}_6\text{H}_6)\text{Ru}(\eta^6\text{-C}_6\text{H}_5\text{Me})]^{2+}$, signals for free benzene and for toluene bound in $[(\eta^6\text{-C}_6\text{H}_5\text{Me})\text{Ru}(\text{H}_2\text{O})_3]^{2+}$ appear. There is no signal at 6.2 ppm for $[\text{Ru}(\eta^6\text{-C}_6\text{H}_6)(\text{H}_2\text{O})_3]^{2+}$. At longer irradiation time, the methyl signal for free toluene increases, indicating formation of the fully solvated complex. Therefore, the reaction sequence is given by



It is known that methyl substituents on Cp in $[\text{CpM}(\eta^6\text{-arene})]^{2+}$ (M = Ru, Fe) increase the covalency of the Cp–Ru bond without activating the Ru–arene bond.¹ We therefore attribute the highly selective cleavage of the Ru–benzene bond in the reaction of II to an enhanced Ru–toluene bond strength, as explained in more detail below.

The release sequence of other compounds was determined in the same manner. The results are shown in Table 2. Obviously, steric reasons alone cannot explain the results. A rationalization

Table 2. Comparison of Calculated Electronic Structure with Observed Sequence of Arene Replacement in the Photochemically Induced Arene Labilization of $[(\text{arene}_1)\text{Ru}(\text{arene}_2)]^{2+}$

compd	arene replaced in (1) ^b	reduced overlap population between fragments ^c		electron distribution in fragments for HOMO/LUMO ^d		
		Ru-C ₆ H ₆	Ru-arene ₂	Ru	C ₆ H ₆	arene ₂
I		0.74		1.9/1.3	0.04/0.3	
II	C ₆ H ₆	<i>0.595</i>	0.604	1.96/1.42	0.02/0.29	0.02/0.29
III	C ₆ H ₆	<i>0.593</i>	0.608	1.96/1.39	0.02/0.29	0.026/0.32
IV	C ₆ H ₆	<i>0.626</i>	0.661	1.95/1.37	0.02/0.28	0.03/0.35
VI	C ₆ Me ₆	0.76				
VII	C ₆ H ₆ /C ₆ H ₅ OMe	<i>0.592</i>	<i>0.591</i>	1.96/1.42	0.02/0.29	0.02/0.3
IX	naphthalene	0.593	0.515	1.96/1.24	0.02/0.24	0.02/0.52
XI ^a	C ₆ H ₆	<i>0.593</i>	<i>0.601</i>	1.96/1.42	0.02/0.3	0.02/0.3

^a $[(\text{C}_6\text{H}_6)\text{Ru}(\text{C}_6\text{H}_5\text{OH})]^{2+}$. By dissolving $[(\text{C}_6\text{H}_6)\text{Ru}(\text{C}_6\text{H}_5\text{Cl})(\text{BF}_4)_2]$ in D₂O. ^b Determined by ¹H-NMR spectroscopy. ^c Italic: predictions for the reaction $[(\text{arene}_1)\text{Ru}(\text{arene}_2)]^{2+} \rightarrow [(\text{arene}_1)\text{Ru}(\text{H}_2\text{O})_3]^{2+} + \text{arene}_2$. ^d Normalized to 2 electrons irrespective of MO occupation.

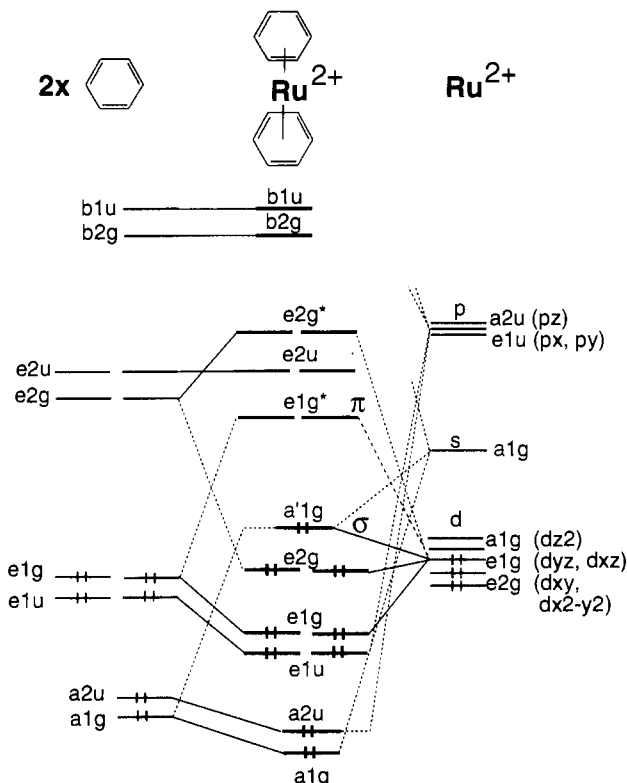
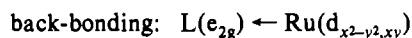
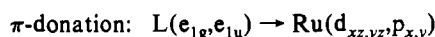
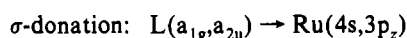


Figure 4. Simplified calculated MO scheme of I in D_{6h} geometry. Solid lines connecting fragment orbitals and molecular orbitals indicate dominant contributions.

is possible on a MO-based approach for the description of the electronic structure in Ru(II) sandwich compounds. Figure 4 shows the calculated MO scheme for I in D_{6h} geometry. The bondings can be described as follows



Although d_{z^2} has a_{1g} symmetry, it acts as a nonbonding MO if its energy is compared to the basic AO in free Ru(II).¹³ Table 2 demonstrates that the HOMO is predominantly metal centered. The LUMO shows a moderate contribution of the ligands which is indifferent to ring tilting. The excitation of an electron from the HOMO to the LUMO is therefore predominantly a d-d transition with a certain MLCT contribution, which will not affect

the bond strength between the metal center and its arene ligands significantly. This description is in good agreement with the magnitude of the molar extinction coefficient and the energy of the lowest energy absorption. The reduced overlap population as a measure for the bonding interaction between Ru and its ligands in the electronic ground state should give appropriate predictions for the reaction sequence, if the solvation process goes via a thermally activated reaction of the electronically excited molecule (a thermally equilibrated triplet state originating from HOMO e_{1g}^*). The important point for the reaction is the generation of an energetically low-lying electron hole on d_{z^2} with excitation. The molecule is then subject to subsequent nucleophilic attack by solvent. Table 2 shows the close agreement between calculated predictions and NMR measurements. The high overlap population in I and VI reflects the very high thermal stability of symmetrical bis(arene) complexes of ruthenium in oxidation state II.¹⁴ Detailed evidence supporting the proposed mechanism will be given in the following sections.

Dependence of Φ_p on λ_{irr} and Steric and Electronic Effects. The quantum yield of the photolysis shows a marked dependence on the irradiation wavelength. Only excitation into the region of the lowest allowed electronic transition leads to significant reaction. Irradiation of I-VII at 458 nm (1000 mW) for 1 h gave virtually no product, because the reactants only absorb very weakly in this region. Excitation with a N₂ laser ($\lambda_{irr} = 337$ nm) resulted in only 3.5% conversion of I after 2.5 h. Intraligand absorbances are therefore not active in the solvation process, probably because they do not mix with the first excited triplet state.

Quantum yields are sensitive to electronic as well as to steric effects. The latter should be predominant if an associative pathway for reaction 1 is involved. As proposed for ruthenium-Cp compounds, methyl-substituted aromatic rings should decrease Φ_p by their donation character and by steric hindrance of incoming solvent molecules. The purely electronic effect upon methylation of the arene rings is given by eq 8 and describes the enhanced

$$\log(k_p/k_{nr}) = \log[\Phi_p/(1 - \Phi_p)] = n\sigma_p + \text{const} \quad (8)$$

competition between more nucleophilic substituted arene ligands and solvent molecules for binding on ruthenium.¹ k_p and k_{nr} are the rate constants for product formation and nonradiative relaxation from the lowest excited triplet state of A back to the ground state, respectively. The Hammett parameter for a methyl group is $\sigma_p = -0.17$ and n equals the number of methyl substituents on the arene ligand. According to the reduced overlap population given in Table 2, the electronic changes in I-VI should be rather small. Comparison of data in Table 2 with eq 8 shows linearity ($R^2 = 0.97$) only up to three methyl substituents, but $\log[\Phi_p/(1 - \Phi_p)]$ is very rapidly decreasing in a nonlinear way for $n > 4$. These results can again be interpreted with a nucleophilic attack on the metal center with important steric hindrance of the

(13) Albright, T. A.; Burdett, J. K.; Whangbo, M.-H. *Orbital Interactions in Chemistry*; Wiley: New York, 1985.

(14) Kaganovich, V. S.; Kudinov, A. R.; Rybinskaya, M. I. *Organomet. Chem. USSR* 1988, 1, 162.

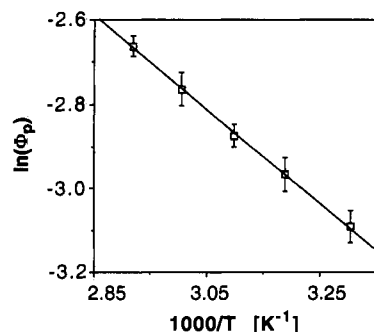


Figure 5. Temperature dependence of the quantum yield Φ_p in the photolysis of $[(C_6H_6)_2Ru](tos)_2$ in 0.05 M H_2SO_4 ($\lambda_{irr} = 351$ nm, 200 mW) in the temperature range 5–45 °C.

incoming solvent molecule at a high degree of substitution of arene ligands.

Temperature and Deuterium Effects on Φ_p . Arrhenius type behavior in the photolysis of I as the tosylate salt in 0.05 M H_2SO_4 (see Figure 5) suggests that a thermally activated reaction of the equilibrated excited state is taking place. A strongly negative activation entropy ΔS^\ddagger is consistent with an associative mechanism. The small activation enthalpy ΔH^\ddagger of 5.4(1) kJ/mol (25 °C) increases slightly with solvent change to DMSO ($\Delta H^\ddagger = 6.1$ (6) kJ/mol), probably due to steric effects.

Φ_p is a function of the rate constant k_p leading to the product and competing radiative (k_r) and nonradiative (k_{nr}) processes. In solution at ambient temperatures k_r can be neglected, since no luminescence was observed. However, temperature-dependent nonradiative multiphonon processes may play a significant role.¹⁵

The comparison of Φ_p for the photolysis of I with that for the photolysis of its perdeuterated analog I- d_{12} is particularly instructive in this respect.¹⁶ For these two compounds Φ_p is identical within experimental error, indicating that the respective values of k_{nr} are approximately equal.

In the weak-coupling case, that is with but a small relative displacement of the potentials of ground and excited states, k_{nr} would be dominated by the highest energy vibration,¹⁷ namely the CH and the CD skeletal vibrations, respectively. Φ_p would then be expected to be considerably enhanced by the perdeuteration. This not being the case, it can be concluded that the nuclear equilibrium configuration of the excited state is strongly distorted with respect to the ground state.¹⁸

Relation between Excited State and Luminescence. Of all of the sandwich compounds of Table 1, VI is the only one to show luminescence at low temperature as a microcrystalline powder or dissolved in PMMA (see Figure 6). Even with I- d_{12} , no luminescence could be observed irrespective of the counterion (BF_4 , PF_6 , tosylate). This confirms the conclusion of the preceding section, because if it were the high-frequency vibrations acting as accepting modes for the radiationless deactivation processes, one would expect the fully deuterated compound I- d_{12} to luminesce rather than the methylated VI. The experimental fact that it is the other way round therefore indicates that steric effects may influence the nonradiative relaxation rates and thus the luminescence lifetimes. The MO scheme for I shows that the first excited state has an $(a_{1g}^1)(e_{1g}^{*1})$ electronic configuration and will thus be Jahn–Teller active. The only energetically low-lying deformation is obtained by tilting the arene ligands. This deformation will be considerably stronger for sterically unhindered complexes and will certainly be restricted in VI. We therefore attribute the luminescence of VI to the conservation of

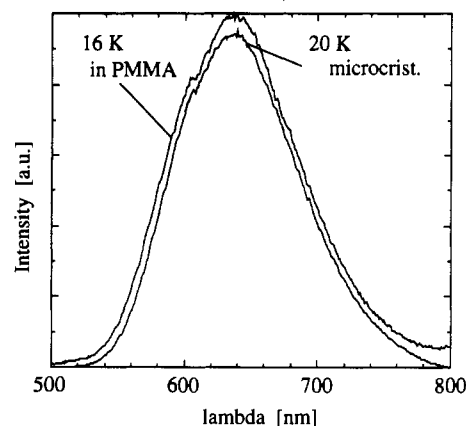


Figure 6. Luminescence spectra of VI at low temperature as a microcrystalline powder and dissolved in PMMA (0.1 wt %).

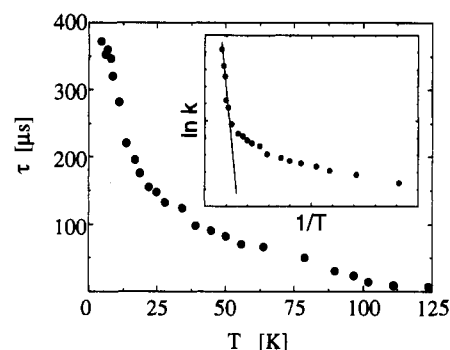


Figure 7. Observed lifetime of the luminescence of VI at 7–125 K. Insert: Arrhenius plot.

the ground-state geometry in the excited state. With all the other systems, ring tilting will lead to a large offset of the potential surfaces, resulting in efficient nonradiative relaxation pathways.

Observed Lifetime. The luminescence of VI shows a non-single-exponential decay in PMMA and as a microcrystalline sample. Such behavior is usually attributed to energy transfer. However, this is also observed in glasses or polymeric matrices in the absence of energy transfer.^{16,19} In particular, large distortions of the excited state lead to a strong coupling to the host system and, in the case of an amorphous matrix, to an inhomogeneous distribution of sites with different relaxation rates.

A mean lifetime was estimated by taking the time for which the initial luminescence intensity had decreased to its $1/e$ value. At 7 K, $\tau_{obs} \approx 400$ μs . Assuming this to be a purely radiative lifetime, the corresponding transition would have an oscillator strength of 2×10^{-5} , which is typical for a parity and spin-forbidden transition of 4d transition metal ions. Therefore the emitting state must have an $\dots(a_{1g}^1)(e_{1g}^{*1})$ configuration.

With rising temperature, the observed lifetimes rapidly decrease to an intermediate plateau at 50–60 K (Figure 7) whereas the luminescence intensity stays approximately constant. Above 70 K, a second decrease of τ_{obs} with a parallel loss of luminescence intensity is observed. This can be explained in terms of a thermal activation of nonradiative processes. An Arrhenius fit to the data in the nonradiative domain ($T = 70$ –125 K) gives an activation energy of 4.13 ± 0.45 kJ/mol. This shows that, even in the sterically hindered VI, only little thermal energy is required to induce nonradiative processes.

Conclusions

The photochemically induced solvation of bis(arene) complexes of Ru(II) can be described by assuming a preequilibrium for the formation of the excited state (see Figure 8). Either relaxation

(15) Petersen, J. D.; Ford, P. C. *J. Phys. Chem.* **1974**, *78*, 1144.

(16) (a) Krausz, E.; Ferguson, J. *Prog. Inorg. Chem.* **1989**, *37*, 293. (b) McClanahan, S. F.; Kincaid, J. R. *J. Am. Chem. Soc.* **1986**, *108*, 3840. (c) Avouris, P.; Gelbart, W. M.; ElSayed, M. A. *Chem. Rev.* **1977**, *77*, 793.

(17) Englman, R.; Jortner, J. *Mol. Phys.* **1970**, *18*, 145.

(18) Gelbart, W. M.; Freed, K. F.; Rice, S. A. *J. Chem. Phys.* **1970**, 2460.

(19) Hauser, A.; Adler, J.; Güttlich, P. *Chem. Phys. Lett.* **1988**, 468.

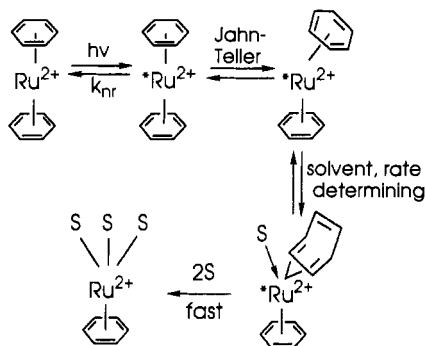


Figure 8. Proposed reaction scheme for the photochemically induced solvation of sandwich compounds.

back to the ground state or distortion to an energetically more favorable geometry follows. The enhanced reactivity of the excited state is due to this structural change and to the generation of an

electron-deficient metal center. The rate-determining step is the subsequent nucleophilic attack of a solvent molecule on ruthenium. The solvolysis is attributed to an associative mechanism involving a transition state, where solvent molecule and arene ligand compete for the bond to ruthenium. The consecutive reaction consists of a fast release of arene and coordination of two more solvent molecules. The proposed mechanism is similar to the one discussed for the related compound $[(\text{Cp})\text{Ru}(\text{arene})]^+$.¹

The properties of the first excited state can be influenced by steric factors. Steric effects are more important in determining the magnitude of the quantum yield than electronic changes induced by σ -donating substituents on the arene ligands.

Acknowledgment. We thank Gabriela Frey for luminescence measurements. We also acknowledge CIBA-GEIGY for elemental analysis and Johnson-Matthey for a loan of RuCl_3 . This work was supported by the Swiss National Science Foundation (Grant No. 20-29585.90).